Demonstration of a single-layer meanderline phase retarder at infrared

Jeffrey S. Tharp, Jose M. Lopez-Alonso, James C. Ginn, and Charles F. Middleton

CREOL College of Optics and Photonics, University of Central Florida, Orlando, Florida 32816

Brian A. Lail

Department of Electrical and Computer Engineering, Florida Institute of Technology, Melbourne, Florida 32901

Ben A. Munk

ElectroScience Laboratory, Ohio State University, Columbus, Ohio 43210

Glenn D. Boreman

CREOL College of Optics and Photonics, University of Central Florida, Orlando, Florida 32816

Received May 4, 2006; revised June 30, 2006; accepted July 3, 2006;
posted July 10, 2006 (Doc. ID 70616); published August 25, 2006

Meanderline wave plates are in common use at radio frequencies as polarization retarders. We present initial results of a gold meanderline structure on a silicon substrate that functions at a wavelength of 10.6 μm in the IR. The measured results show a distinct change in the polarization state of the incident beam after passing through the device, inducing a 74° phase retardance between horizontal and vertical components. A high degree of polarization (88%) is maintained in the transmitted beam with an overall power transmittance of 38% and a beam profile that remains essentially unchanged. © 2006 Optical Society of America

OCIS codes: 260.1440, 260.5430.

Meanderline wave plates have traditionally been used to convert linearly polarized radiation into circularly polarized radiation. The meanderline structure acts as a phase retarder for the two orthogonal wave components of an incident electric field. These two orthogonal components lie along the meander axis and perpendicular to the meander axis. The meander structure acts primarily as an inductive element along the meander axis and a capacitive element perpendicular to the meander axis, leading to a relative phase delay. Such structures are commonplace in the rf portion of the spectrum.[1–4] Advances in lithography have made such structures feasible in the IR and terahertz portions of the spectrum. The ease of fabrication, low fabrication costs, and compact construction may provide a potentially important alternative to birefringent crystals or prism retarders in these bands.

The present proof-of-concept demonstration at IR is significant because it shows that such structures can be scaled down to small dimensions. Further, the high-frequency properties of metals, while not as ideal as in the rf, do allow devices of viable performance to be constructed. In particular, our present measured values for depolarization and throughput are valuable benchmarks for future device development.

As a starting point for the designed meanderline to operate at 10.6 μm, we scaled down a published rf design proportionally to the decrease in wavelength.[5] We then refined our design and modeled its performance using Ohio State's Periodic Method of Moments (PMM) solver, which uses a single unit cell to simulate an infinite array by the application of mutual-impedance and plane-wave-expansion techniques. The PMM solver was also configured with an outside MatLab program that allows the use of frequency-dependent complex permittivities, the input data for which are measured using ellipsometric techniques.[6] The expected performance for the design was cast in terms of the axial ratio (AR) the (ratio of major to minor axes of the polarization ellipse) of the electric field transmitted through the structure, and also the relative phase delay between the transmitted orthogonal components. Circular polarization would thus have an AR of 1 and a relative phase delay of ±90°.

The design variables explored were the geometrical dimensions of the meanderline structure including: meanderline width (w), pulse width (pw), pulse height (ph), and periodicity (dx). The parameters for this design were 0.4, 1, 1, and 2.3 μm, respectively, and are shown in an electron micrograph of the fabricated array in Fig. 1(a). This design was expected to produce radiation with an AR of 2.0 and a relative phase delay of 64° at 10.6 μm as shown in Fig. 1(b).

Fabrication of the IR meanderlines was accomplished using electron-beam lithography on a high-resistivity (3–5 kΩ cm) silicon wafer. The high-resistivity silicon wafer was considered necessary because the function of the meanderlines depends upon electrical insulation between them. Also the high-resistivity silicon had negligible material attenuation at 10.6 μm. The meander structure needed to be of a conductive material at IR frequencies to minimize ohmic losses. We used gold at a thickness of 100 nm. The overall dimensions of the array were 1 cm $\times$ 1 cm.

We characterize the polarization change caused by the meanderlines using the Stokes parameters of the

0146-9592/06/180001-0/$15.00

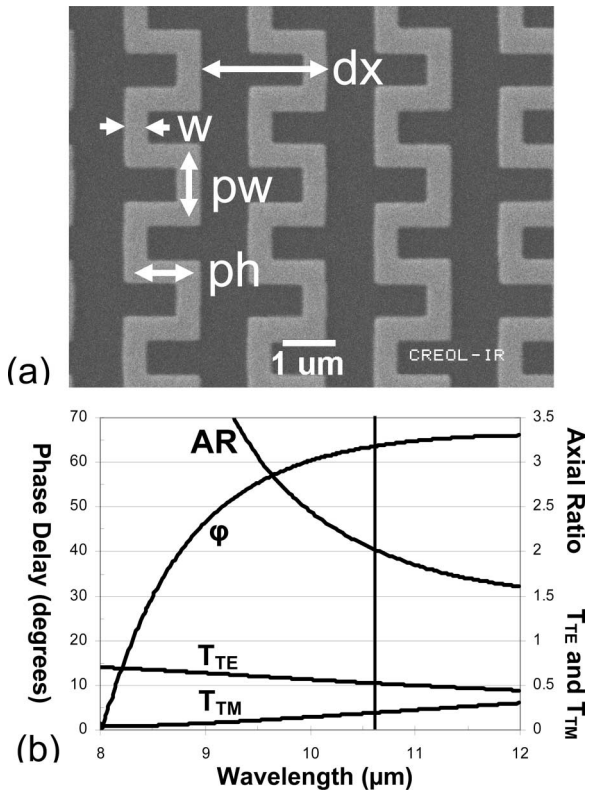

Fig. 1. (a) Electron micrograph image of the fabricated gold meanderline structure on a high-resistivity silicon substrate and (b) the expected phase delay (φ), axial ratio (AR), and power transmission coefficients (T_{TE} and T_{TE}) as modeled in PMM with a marker at 10.6 μm for comparison to the measured data.

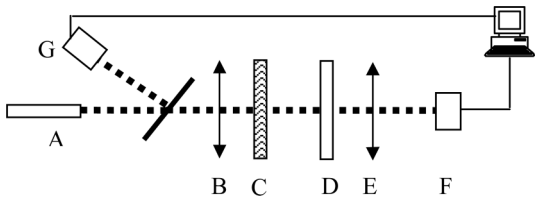

Fig. 2. Schematic of the experimental setup: A, CO_2 laser; B, wire-grid linear polarizer; C, meanderline; D, quarter-wave plate; E, analyzing polarizer; F and G, signal and reference detectors connected to a computer for data acquisition.

input and output beams. Our experimental setup, shown in Fig. 2, included a linearly polarized CO_2 laser beam, two BaF_2 wire-grid polarizers, and a quarter-wave plate. Two thermal detectors were used, with one used to calibrate out laser-power fluctuations. The Stokes parameters were determined, in the usual way, through a set of power measurements. The first power measurements were made without the quarter-wave plate in the optical train and with the analyzing polarizer rotated from 0° to 360°. The resulting dependence of received power as a function of the analyzing polarizer angle was fitted to a periodic function, and I_0, I_{45}, and I_{90} were determined from the fitted curve. The other power measurement was with the quarter-wave retarder in the optical train (fast axis horizontal) and the analyzing polarizer at 45° producing the value I_{q45}. The Stokes parameters were then calculated using[7]

$$S_0 = I_0 + I_{90}, \quad S_1 = I_0 - I_{90}, \quad S_2 = 2I_{45} - S_0,$$

$$S_3 = 2I_{q45} - S_0. \tag{1}$$

The Stokes parameters are then used to determine the orientation (ψ) and the AR of the polarization ellipse using

$$\tan(2\psi) = S_3/S_0, \quad \mathrm{AR} = 1/\left\{\tan\left[\tfrac{1}{2}\sin^{-1}(S_3/S_1)\right]\right\}. \tag{2}$$

From the standard deviation of the power measurements with respect to the fitted curve the uncertainty in the retardance, Stokes parameters, orientation, and AR can be calculated.[8] The numerical results are shown in Table 1. They show a drastic change in the polarization state of the radiation after passing through the single-layer meanderline structure. The AR of the polarization ellipse changed from its initial linear polarization to elliptical polarization with an AR of 2.51±0.05, while the orientation of the ellipse changed from 43.5°±0.4° to 9.1°±0.5° after passing through the meanderline (Fig. 3). Another interesting aspect is that the degree of polarization of the incident radiation was measured to be 0.98, while the degree of polarization after passing through the meanderline was 0.88. Therefore the meanderline changed the state of the polarization with little degradation to the degree of polarization.

The power throughput was measured to be 38% with this design. The power losses included a dielectric reflection loss of 45% and a structure loss of 17%. The power transmission coefficients for radiation polarized along and perpendicular to the meander axis (T_{TE} and T_{TM}), were measured to be 0.13 and 0.56 at 10.6 μm, respectively. These measured values compare well with the PMM modeled values (0.19 and 0.52) for these transmission coefficients, shown as a function of wavelength in Fig. 1(b). We believe that the loss due to the meanderline structure can be attributed to ohmic losses in the gold and to backscatter of the power due to reradiation from the structure.[5]

Table 1. Stokes Parameters and Polarization-Ellipse Parameters for the Incident and Transmitted Beams

Stokes Parameters	Incident Beam	Transmitted Beam
S_0	1.000	1.000
S_1	0.043±0.014	0.546±0.003
S_2	1.007±0.016	0.193±0.010
S_3	−0.019±0.010	0.672±0.011
Ψ (orientation)	43.5°±0.4°	9.15°±0.44°
AR (axial ratio)	111	2.51±0.05

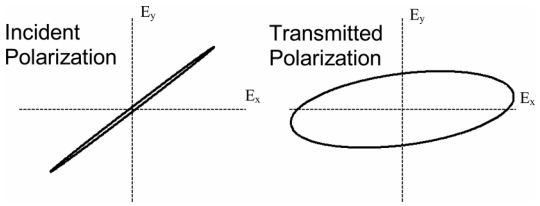

Fig. 3. Polarization ellipses for incident beam (left) and transmitted beam (right).

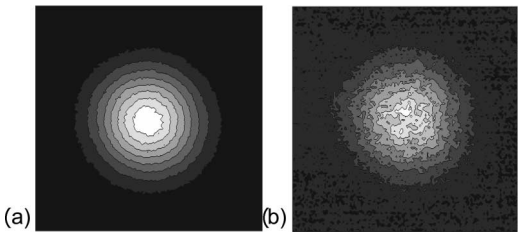

Fig. 4. Beam contours (a) before and (b) after the meanderline.

We also determined the orthogonal-component relative phase delay of the meanderline structure using

$$\varphi = \tan^{-1}(S_3/S_2). \tag{3}$$

The phase delay (φ), as measured, was $74.0° \pm 1.0°$.

The present discrepancies between the expected values of the AR (2.51 versus 2.0) and the relative phase delay (74° versus 64°) can perhaps be attributed to the fact that the PMM solver used a specification of sheet resistance for the metals rather than a volumetric resistance, which may not be accurate for the small thicknesses used since the geometry itself will contribute to the resistance. We will continue to investigate more sophisticated modeling techniques to achieve better agreement between modeling and measurements.

The incident and transmitted beam profiles of the meanderline retarder were measured using a Spiricon pyroelectric camera. The measured beam profiles are shown in Fig. 4, with the result that the meanderline retarder did not significantly alter the beam profile other than the overall intensity.

To our knowledge, this is the first proof of concept of a meanderline structure functioning in the IR. We fabricated a single-layer gold meanderline on a high-resistivity silicon substrate. This structure changed the polarization state of the radiation from linear polarization at $43.5° \pm 0.4°$ to elliptical polarization with an AR of 2.51 ± 0.05 and a relative phase delay of $74° \pm 1.0°$. Moreover, the degree of polarization is minimally affected, suggesting that the change of polarization is caused by the meanderline phase delay and not by scattering.

The throughput of the single-layer meanderline retarder is 38%, which is low compared with commercially available quarter-wave plates, which typically have a throughput of approximately 90% at the design wavelength. We are at present involved in research aimed at improving the transmittance of the meanderline structure. The reflection losses can be reduced by use of low-refractive-index substrates, or perhaps by implementation of antireflection coatings on the substrate. However, any such coating on a surface that is in contact with the meanderlines will affect the design. Ohmic losses may be lowered somewhat by optimization of the metal thickness, which has the potential to change the impedance of the meanderlines. Reradiation losses may perhaps be lowered by the use of multiple meanderline layers, but at the expense of a more complex structure. If it is indeed possible to increase the throughput, the meanderline-retarder approach stands to have some significant advantages compared with crystalline wave plates, at least in the IR and terahertz ranges. Commercially available crystalline wave plates are typically designed for operation only at specific laser wavelengths, because the physical thickness of the crystals directly impacts the design. Alternatively, the meanderline can be easily designed and fabricated to operate at any arbitrary wavelength of interest by varying the geometry. The meanderline also has the advantages of weight and compactness, reduced optical path, and simplicity of fabrication within the performance limits of lithography.

This work was supported by the U.S. Department of Energy, under research contract 00046731 from the Idaho National Laboratory, and by a research contract from DRS Optronics, Melbourne, Florida. Additional support was provided by the Florida High Tech Corridor Council. J. Tharp's e-mail address is jstharp@creol.ucf.edu.

References

1. L. Young, L. Robinson, and C. Hacking, IEEE Trans. Antennas Propag. **21**, 376 (1973).
2. M. Mazur and W. Zieniutycz, in *13th International Conference on Microwaves, Radar, and Wireless Communications* (IEEE, 2000), Vol. 1, pp. 78–81.
3. J. Zürcher, Microwave Opt. Technol. Lett. **18**, 320–323 (1998).
4. T. K. Wu, IEEE Microw. Guid. Wave Lett. **4**, 199 (1994).
5. B. A. Munk, *Finite Antenna Arrays and FSS* (Wiley-IEEE, 2003), Appendix C.
6. J. Ginn, B. Lail, D. Shelton, J. Tharp, W. Folks, and G. Boreman, in *22nd International Review of Progress in Applied Computational Electromagnetics* (ACES, 2006), pp. 307–311.
7. D. Goldstein, *Polarized Light*, 2nd ed. (Dekker, 2003).
8. *Guide to the Expression of Uncertainty in Measurement*, 2nd ed. (International Organization for Standardization, 1995).